Carbohydrate Polymers 117 (2015) 70–77

Contents lists available at ScienceDirect

Carbohydrate Polymers

journal homepage: www.elsevier.com/locate/carbpol

Mechanism of Au(III) reduction by chitosan: Comprehensive study with ^{13}C and ^{1}H NMR analysis of chitosan degradation products

Alexander Pestov[a], Alexander Nazirov[b], Evgeny Modin[c], Alexander Mironenko[b], Svetlana Bratskaya[b,*]

[a] I. Ya. Postovsky Institute of Organic Synthesis, Ural Branch of RAS, 20, S. Kovalevskoy str., Yekaterinburg 620990, Russia
[b] Institute of Chemistry, Far East Branch of RAS, 159, prosp.100-letiya Vladivostoka, Vladivostok 690022, Russia
[c] Far Eastern Federal University, 8, Sukhanova St., Vladivostok 690950, Russia

ARTICLE INFO

Article history:
Received 31 July 2014
Received in revised form 9 September 2014
Accepted 11 September 2014
Available online 28 September 2014

Keywords:
Chitosan
Gold nanoparticles
Metal/polymer ratio
Decarboxylation
Depolymerization
Formate

ABSTRACT

The mechanism of Au(III) reduction by chitosan has been proposed on the basis of comprehensive study of kinetics of Au(III) reduction and chitosan chain degradation using UV–vis spectroscopy and viscosimetry, and identification of reaction products using colloid titration and ^{13}C, ^{1}H NMR spectroscopy. We have shown that formation of gold nanoparticles in $H[AuCl_4]$/chitosan solutions starts with hydrolysis of chitosan catalyzed by Au(III). The products of chitosan hydrolysis rather than chitosan itself act as the main reducing species. According to ^{13}C and ^{1}H NMR spectroscopy data, chitosan/Au(0) composites contain chitosan with reduced molecular weight and acetylation degree, whereas water-soluble by-products consist of chitosan oligomers with higher acetylation degree, derivatives of glucosamine acids, and formate ion. Chitosan degradation has significantly contributed to the decrease of its efficiency as a gold nanoparticles stabilizer. The gold particle size increased from 6.9 nm to 16.2 nm, when Au(III)/chitosan molar ratio changed from 1:80 to 1:10.

1. Introduction

Biogenic synthesis of metal nanoparticles as well as metal ions reduction using biopolymers attract an increasing interest due to their compliance with the principles of "green" chemistry, non-toxicity, and biocompatibility of the fabricated materials (Kumar & Yadav, 2009; Park, Hong, Weyers, Kim, & Linhardt, 2011; Wu et al., 2014). A wide range of biopolymer/metal nanoparticles composites, first of all, those containing gold and silver, are applied in versatile fields from drug delivery and photothermal therapy to sensing (Agrawal, Strijkers, & Nicolay, 2010; Chen, Wang, Chen, Xu, & Liu, 2013; Kumar & Yadav, 2009; Zhang, Sun, Jasinski, Patel, & Gobin, 2012). Due to their availability, relatively low cost, and multi-functionality, polysaccharides became the most extensively investigated class of natural polymers used as reducing and/or stabilizing agents in synthesis of polymer/gold nanoparticles composites (Djoković et al., 2011; Huang, Yuan, & Yang, 2004). Among all polysaccharides, chitosan composed of β-(1-4)-linked D-glucosamine and *N*-acetyl-D-glucosamine has gained the highest popularity. The polycation nature of chitosan is particularly favorable for gold nanoparticles synthesis, since, on the one hand, chitosan can effectively bind $[AuCl_4]^-$ ions (Di Carlo et al., 2012; Huang et al., 2004), which is important to control rate of nucleation and nanoparticles growth (Mayer & Mark, 1998), and, on the other hand, it can stabilize nanoparticles formed thanks to high affinity of N-containing functional groups to the surface of metallic gold (Murugadoss & Sakurai, 2011; Tiwari, Mishra, Mishra, Arotiba, & Mamba, 2011).

It was shown that varying synthesis parameters, such as concentration of chitosan (Huang & Yang, 2004; Huang et al., 2004) and Au(III) ions (Huang et al., 2004), chitosan molecular weight (Huang & Yang, 2004), pH and Au(III) speciation (Vo, Guillon, Dupont, Kowandy, & Coqueret, 2014), number of carboxylic groups, and dissociation degree of organic acid, in which chitosan is dissolved (Di Carlo et al., 2012), enabled one to obtain gold nanoparticles of various shapes and sizes. However, up to now neither the mechanism of Au(III) ions reduction by chitosan nor the chemical structure of the reaction by-products has been investigated in detail. The most important recent studies demonstrated that "green" synthesis of gold nanoparticles in chitosan solution is accompanied by degradation of chitosan chains (Sun et al., 2008), while chitosan/Au(III) complexation plays a significant role in this process (Vo et al., 2014).

* Corresponding author. Tel.: +7 423 2215295; fax: +7 423 2311889.
E-mail address: sbratska@ich.dvo.ru (S. Bratskaya).

http://dx.doi.org/10.1016/j.carbpol.2014.09.030
0144-8617/

However, the products of chitosan oxidation by Au(III) have not been identified, and the effect of the Au(III)/chitosan ratio on morphology and chemical composition of Au(0)/chitosan particles have not been investigated.

Gaining information on mechanism of Au(III) "green" reduction is important for understanding how chitosan characteristics, which can differ significantly from one source to another, affect properties of gold/chitosan composites. Moreover, in the light of expanding application of chitosan/gold composites in biomedical field, it is crucial to avoid overestimation of biocompatibility of the obtained composites, which obviously contain not only the biocompatible chitosan, but also unknown yet products of its oxidation.

The main objective of the present work was to investigate the mechanism of Au(III) reduction by chitosan using ^{1}H and ^{13}C NMR spectroscopy for identification of the reaction products and to show how the metal loading, i.e., the Au(III)/chitosan ratio, affects kinetics of Au(III) reduction, chitosan chain degradation, as well as morphology of the Au(0)/chitosan particles and final chemical composition of the systems.

2. Experimental

2.1. Materials and reagents

Medium molecular weight chitosan (MMW) with a deacetylation degree of 88% (^{1}H NMR data) and a molecular weight of $\sim 5 \times 10^{5}$ Da was purchased from JSC "Bioprogress" (Russia). Chitosan stock solutions with concentration 0.1% was prepared by dissolution of the required amount of polymer in 0.1% acetic acid solution. $H[AuCl_4]$ solution of a concentration of 0.01 mol/L was prepared by dissolution of an appropriate amount of gold foil in aqua regia followed by three cycles of evaporation/addition of concentrated HCl. The resulting concentration of HCl in $H[AuCl_4]$ stock solution was 0.045 mol/L.

2.2. Au(III) reduction in chitosan solutions

Stock solution of $H[AuCl_4]$ was added into freshly prepared chitosan solutions to yield Au(III)/chitosan molar ratios of 1:10, 1:20, 1:40, and 1:80. The Au(III)/chitosan molar ratio (R) was calculated taking into account that chitosan is composed of glucosamine and *N*-acetyl-glucosamine units:

$$R = \frac{\left(m_{Au}/Ar_{Au}\right)}{\left(m_{chit}/\left(0.88 \times Mr_{Glc} + 0.12 \times Mr_{GlcNAc}\right)\right)},$$

where m_{Au}, m_{chit}—weights of Au and chitosan, respectively, Mr_{Glc} and Mr_{GlcNAc}—molecular weights of glucosamine and *N*-acetyl-glucosamine.

The mixtures were permanently stirred and kept at 25 °C until the constant value of the optical density was reached. Formation of colloidal gold was monitored using an UV-1650PC spectrophotometer (Shimadzu, Japan). Au(III) to Au(0) conversion degree (CD_{Au}) was calculated according to the formula:

$$CD_{Au} = 1 - \left(\frac{(A_t - A_0)}{(A_{max} - A_0)}\right),$$

where A_0 and A_t—the optical densities of chitosan solution immediately after addition of $H[AuCl_4]$ and after the fixed time (t), respectively; A_{max}—the maximum optical density reached (optical densities were determined at the wavelength of plasmon absorption band).

After completion of Au(III) reduction, the chitosan/Au(0) composites varying in metal/polymer ratios were precipitated by adjusting pH to 10.0 with NaOH solution, centrifuged at 4400 rpm (Eppendorf 5702R centrifuge), immediately thoroughly washed with distilled water and acetone and dried under room temperature. The gold content in supernatant was below detection limit of atomic absorption spectroscopy (Solaar 6 M, Thermo) indicating that more than 99% of gold was precipitated in a form of Au(0)/chitosan composite. The chitosan weight loss (%) in composite was calculated as:

$$\Delta W_{chitosan} = \left(1 - \frac{W_{composite} - W_{Au}}{W_{chitosan}}\right) \times 100\%,$$

where $W_{composite}$—the weight of the precipitated composite, W_{Au} and $W_{chitosan}$—total weights of gold and chitosan used for composite preparation, respectively.

^{13}C and ^{1}H NMR spectra of the composite with the Au/chitosan molar ratio 1:10 were recorded as described below: ^{1}H NMR (D_2O/DCl, 500 MHz): δ 2.09 (3*H*, br s, CH_3), 3.24 (1*H*, br t, *H*-2 $GlcNH_2$), 3.78–3.94 (5*H*, m, *H*-2,3,4,5,6), 4.94 (1*H*, br d, *H*-1 $GlcNH_2$)—Fig. S3; ^{13}C NMR (D_2O/DCl, 126 MHz): δ 24.7 (s, CH_3), 58.2 (s, C2), 62.7 (s, C6), 72.7 (s, C3), 77.4 (s, C5), 79.1 (s, C4), 100.1 (s, C1 of $GlcNH_2$), 103.9 (s, C1 of $GlcNHCOCH_3$), 177.3 (s, C=O)—Fig. S4. Upon precipitation of the composite with the Au/chitosan molar ratio 1:10, the supernatant was dried at 40 °C in a convection oven and analyzed by ^{1}H NMR spectroscopy: ^{1}H NMR (D_2O/DCl, 500 MHz): δ 1.90 (3*H*, br s, CH_3COO), 2.05 (3*H*, br s, CH_3), 2.70 (2*H*, m, *H*-2 $GlcNH_2$, $CH(NH_2)COO$), 3.38–3.93 (m, *H*-2,3,4,5,6), 4.45 (1*H*, br d, *H*-1 $GlcNH_2$), 4.58 (1*H*, br d, *H*-1 $GlcNHCOCH_3$), 8.44 (1*H*, s, *H*COO)—Fig. S5.

2.3. ^{1}H and ^{13}C NMR spectroscopy

^{1}H and ^{13}C NMR spectra were recorded on a Bruker AVANCE-500 spectrometer at 70 °C to increase the solubility of samples and attain better resolution of the signals. Samples were dissolved in 0.5 M solution of DCl in D_2O (concentration of polymer was 10 mg/mL); sodium 3-(trimethylsilyl)-1-propanesulfonate (DSS) was used as an internal standard. Suppression of the solvent signal during the spectrum recording was realized by the presaturation sequence.

2.4. Rheological measurements

Strain rate-controlled rheological tests in the shear rate range from 1 up to 1000 s^{-1} were performed at 25 °C on a Physica MCR 301 rheometer (Anton Paar, Austria) equipped with a 50 mm diameter cone-plate measuring system. The typical flow curves are presented in Fig. S1 (Supporting materials). To simplify the data presentation, the changes in the chitosan/Au(III)/Au(0) solutions viscosity were monitored at a shear rate of 100 s^{-1}. The viscosity of the chitosan solution with the HCl concentration corresponding to that in the composite solution with the Au(III)/chitosan molar ratio 1:20 was monitored under the same conditions.

The viscosity conversion degree ($CD_{viscosity}$) was calculated according to the formula:

$$CD_{viscosity} = \frac{(\eta_0 - \eta_t)}{(\eta_0 - \eta_{min})},$$

where η_0 and η_t—the viscosity of the chitosan solution immediately after addition of $H[AuCl_4]$ and after the fixed time (t), respectively; η_{min}—the minimum viscosity reached (corresponds to the maximum optical density reached).

2.5. Transmission electron microscopy (TEM)

Samples were prepared by dropping diluted Au(0)/chitosan composite solutions onto the copper grid coated with a Formvar film. TEM images were obtained using a Carl Zeiss Libra 200

FE transmission electron microscope at an accelerating voltage of 200 kV in the bright field mode. To gain the required statistical data, the mode of image matching was used: panoramic images of 4×4 frames of total area of 3.3×3.5 μm were obtained. TEM images processing for calculating the particles number and sizes was carried out using the ImageJ software (Schneider, Rasband, & Eliceiri, 2012). The images contrast was increased by histogram normalization or adjustment. The area of interest was segmented through the image binarization: overlapping particles were marked out using the watershed segmentation algorithm.

2.6. Colloid titration

The content of anionic and cationic colloidal species in supernatants upon Au(0)/chitosan composites precipitation were determined by colloid titration at pH 8.2 and 2.5, respectively, using a PCD-03 particle charge detector (Mütek, Germany). Solutions of sodium polyethylene sulfonate (PES-Na) and polydiallyldimethylammonium chloride (PDADMAC) were used as titrants. The concentrations of colloidal species (CCS, meqv/L) were calculated according to the formula:

$$\mathrm{CCS} = \frac{C_{\mathrm{titrant}} \times V_{\mathrm{titrant}}}{V},$$

where C_{titrant} —the PES-Na or PDADMAC concentration (meqv/L), V—the volume of titrated solution (L), V_{titrant}—the equivalent titrant volume (L).

The weight% of chitosan decomposed to "cationic trash" (positively charged colloids, which do not precipitate in alkaline media) was calculated as:

$$\Delta W_{\mathrm{cationic}} = \frac{\mathrm{CCS}_{\mathrm{cationic}}}{\mathrm{CCS}_{\mathrm{chitosan}}} \times 100,$$

where $\mathrm{CCS}_{\mathrm{cationic}}$—the concentration of colloidal species (meqv/L) in supernatant solution upon precipitation of the chitosan/Au(0) composite, $\mathrm{CCS}_{\mathrm{chitosan}}$—the concentration of colloidal species (meqv/L) in 0.1% chitosan solution. The weight% of chitosan decomposed to "anionic trash" ($\Delta W_{\mathrm{anionic}}$) was calculated accordingly.

The weight% of chitosan decomposed to low molecular weight products (LMW—water-soluble reaction products, which do not have colloid properties and cannot be determined by colloid titration) was calculated as:

$$\Delta W_{\mathrm{LMW}} = \Delta W_{\mathrm{chitosan}} - \Delta W_{\mathrm{cationic}} - \Delta W_{\mathrm{anionic}}$$

3. Results and discussion

3.1. Influence of metal/polymer ratio on kinetics of Au(III) reduction by chitosan

It was previously shown that the size and stability of polysaccharide/gold composite obtained either with addition of reducing agents (Murugadoss & Sakurai, 2011) or without them (Huang & Yang, 2004; Pal, Esumi, & Pal, 2005) depend on the metal ion to polymer ratio. However, the effect of Au(III)/chitosan ratio on properties of gold nanoparticles has been investigated mainly at fixed metal ion concentration and varied concentration of chitosan. Obviously, under these conditions, the nucleation and growth of nanoparticles are to a great extend controlled by the system viscosity. At the same time, since the maximal metal loading in a polymer/gold composite is an important characteristic of the efficiency of polymers as reducing agents and stabilizers (Mayer & Mark, 1998; Murugadoss & Sakurai, 2011), it is important to understand, which factors limit the stability of chitosan/gold nanoparticles obtained by "green" method at fixed polymer concentration.

Upon addition of $H[AuCl_4]$ to chitosan solution at room temperature, yellow color of the system immediately disappears due to dissociation of complex ion $[AuCl_4]^-$ and formation of a new complex Au(III)/chitosan for all studied metal/polymer ratios. These changes are accompanied by the decrease of the absorption peak in the UV–vis spectrum at $\lambda = 313$ nm corresponding to metal–ligand charge transfer in $[AuCl_4]^-$ (Fig.S2, Supporting materials). Similar effect was previously observed in solutions of alginic acid (Pal et al., 2005) and related to formation of Au(III)/alginic chelates. Very recently, Vo et al. (2014) proved that chitosan could coordinate Au(III) ions via substitution of Cl^- ions by chitosan N or O atoms in inner sphere of $[AuCl_4]^-$ complex, although the methods used have not allowed an unambiguous conclusion on the complexation mode and the involvement of O atoms of chitosan. We assume that, most likely, chitosan/Au(III) coordination occurs with participation of O atom of glycoside bond resulting in formation of complex of structure I (Scheme 1).

Kinetic investigations of Au(III) reduction at different $[AuCl_4]^-$/chitosan ratios have revealed several interesting features. New peaks corresponding to plasmon adsorption of gold nanoparticles appear only 120–180 min upon addition of $H[AuCl_4]$ to chitosan solution; and the induction period (time before formation of purple colloidal gold) increases along with the increasing $H[AuCl_4]$/chitosan ratio (Fig. 1A and B).

Already at the early stages of colloidal gold formation, the maximum of plasmon adsorption band clearly depends on the Au(III)/chitosan molar ratio and shifts from 520 nm (ratio 1:40) to 530 nm (ratio 1:10)—Fig. 1E.

In accordance with the known dependence of plasmon band wavelength on gold nanoparticles size (Khlebtsov, 2008), such spectral changes can be attributed to formation of larger gold nanoparticles, when the Au(III) content in the composite increases. Interestingly, the stage of nanoparticles growth accompanied by the increase of wavelength of plasmon adsorption is followed by notable decrease in apparent gold nanoparticles size (Fig. 1E) that can be explained either by particles recombination or changes in the particles morphology.

At the final stage of Au(III) reduction, the maxima of plasmon adsorption in chitosan/Au(0) composites spectra were located at 536 nm, 530 nm, 527 nm, and 525 nm for $H[AuCl_4]$/chitosan molar ratios 1:10, 1:20, 1:40, and 1:80, respectively (Fig. 1F). The absence of the long-wavelength wing in UV–vis spectra confirms that gold nanoparticles were not aggregated and, therefore, at the higher gold concentration plasmon band shifts mainly due to the increased particle size. This conclusion is supported by TEM images of chitosan/Au(0) composites formed at various $[AuCl_4]^-$/chitosan ratios (Fig. 2), which show increase of the average gold particle size and broadening of size distribution with increase of metal loading. Moreover, particles of non-spherical shape are formed at high metal loading (ratios 1:10 and 1:20). Starting from $H[AuCl_4]$/chitosan molar ratio 1:40, further decrease of the metal loading does not influence the size and shape of gold nanoparticles in composite-spherical particles of an average of size 6.9 nm are formed. The size of the particles formed was smaller and polydispersity was significantly lower as compared to Au(III) "green" reduction with chitosan at elevated temperature (Sun et al., 2008).

Dramatic decrease of the chitosan solutions viscosity was observed within 1000 min starting from $H[AuCl_4]$ addition (Fig. 1C). Comparison of Au(III) to Au(0) conversion degree curves (Fig. 1B) with corresponding changes in viscosity (Fig. 1C and D) reveals that viscosity drops at least twice when only 5–15% of Au(III) is converted to Au(0). Moreover, the viscosity drop becomes more significant with the increase of gold concentration in solution, i.e. metal loading in composite. It is worth mentioning that these changes in viscosity are directly related to the presence of $H[AuCl_4]$,

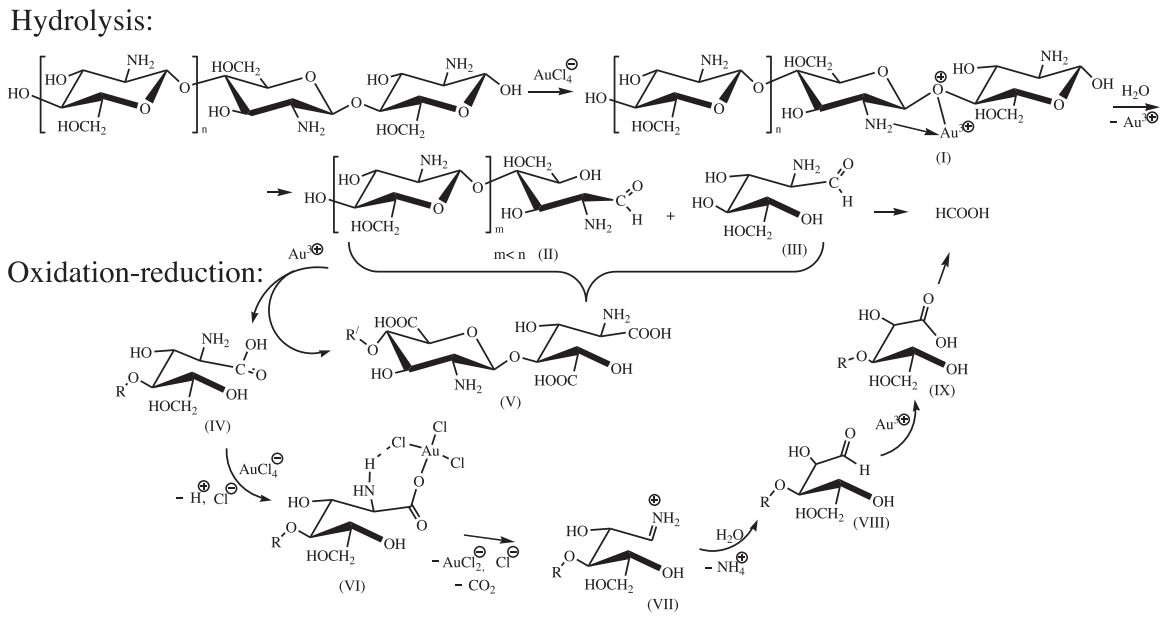

Scheme 1. Chitosan transformations in reaction with Au(III) ions.

since the viscosity of chitosan solution remained constant for several days after addition of HCl in the amount corresponding to that in $H[AuCl_4]$/chitosan mixtures (Fig. 1C).

The rheological data obtained at all metal/polymer ratios support the hypothesis that the reduction of Au(III) with chitosan is accompanied by degradation of the macromolecular chain made by Sun et al. (2008). However, shortening of chitosan chain is obviously not the final stage of its oxidative degradation. We have found significant weight loss of composites increasing along with the increase of metal loadings that could result only from decomposition of chitosan to water soluble products (Table 1). This conclusion is based on two facts: (i) quantitative precipitation of gold nanoparticles with chitosan in alkaline media was corroborated by the atomic adsorption analysis, (ii) medium and high molecular weight chitosans and their composites with gold nanoparticles can be quantitatively precipitated in alkaline media.

To shed the light on the mechanism of Au(III) reduction with chitosan, the compositions of precipitated Au(0)/chitosan particles and soluble reaction products were analyzed using ^1H and ^{13}C NMR spectroscopy. As a complementary technique, colloid titration was used to determine the content and charge of water-soluble "colloidal trash" in supernatant after precipitation of chitosan/Au(0) composite.

3.2. ^1H and ^{13}C NMR identification of chitosan oxidative degradation products

Analysis of precipitated chitosan/Au(0) composite (metal/polymer ratio 1:10) by ^1H and ^{13}C NMR spectroscopy reveals that the organic part in composite is represented by chitosan, whose acetylation degree determined from ratio of integral intensities of signals H atoms at 2.06 ppm (CH_3) and 3.23 ppm. (H-2) was lower (0.08) than in original chitosan (0.12). Signals in the ^1H NMR spectrum of chitosan/Au(0) composite (Fig. 3) are notably better resolved compared to signals in the original chitosan spectrum (see details in Fig. S3, Supporting materials) that is a sign of decrease of chitosan molecular weight during Au(III) reduction. Besides, very low intensity signal, corresponding to the H-atom in hemiacetal group, appears at 5.45 ppm. Most likely, such groups are located at C-1 atoms of terminal *N*-acetylglucosamine units. Thus, the ^1H NMR data (Fig. 3) support the viscometry data on hydrolytic destruction of chitosan chain: the number of sugar units at the free reducing end increases, therefore, the number of H-1 atoms decreases.

The weight loss of chitosan/Au(0) composite remarkable decreases solution viscosity and lowers apparent molecular weight of chitosan confirming degradation of chitosan to low molecular weight water-soluble products in the Au(III) reduction process. Analysis of the supernatant solution after precipitation of the chitosan/Au(0) composite by ^1H NMR spectroscopy (Fig.S5, Supporting materials) has shown the presence of chitosan with the increased acetylation degree (0.26) and formate ions (signal at 8.44 ppm), the ratio formate/amino-group was 9:1. A new group of signals, which are not typical for chitosan but were compatible with signals of glucosamine acids (Pretsch, Bühlmann, & Affolter, 2000; Whittall & Sutton, 2009), appeared at 2.70–3.70 ppm.

3.3. Mechanism of Au(III) reduction with chitosan

Taking into account the viscosimetric, spectrophotometric data and the results of ^1H and ^{13}C NMR analysis of reaction products, the following mechanism of Au(III) reduction with chitosan at room temperature can be proposed.

Au(III) ion as a strong Lewis acid, which actively promotes intra- or intermolecular attacks of a nucleophile (Soriano & Marco-Contelles, 2011), initiates catalytic hydrolysis of chitosan macromolecular chain (Scheme 1) that leads to remarkable viscosity decrease. Immediately upon mixing $H[AuCl_4]$ and chitosan solution, the absorption band at 313 nm disappears indicating to dissociation of $[AuCl_4]^-$complex and formation of Au(III)-chitosan complex (I, Scheme 1). Our data support the hypothesis made recently by Vo et al. (2014) that complexation of Au(III) with glucosamine moieties could activate the reducing function of chitosan. However, we believe that involvement of glycoside oxygen atom to Au(III) coordination yielding the structure I (Scheme 1) is more likely compared to coordination with C-3 hydroxyl oxygen suggested by Vo et al. (2014). Glycosidic oxygen has been previously identified as a possible binding site for transition metal ions using DFT calculations (Braier & Jishi, 2000). Moreover, protonation of the glycosidic oxygen atom with formation of conjugated acid followed by heterolysis of endocyclic O-5 and C-1 bonds is the most

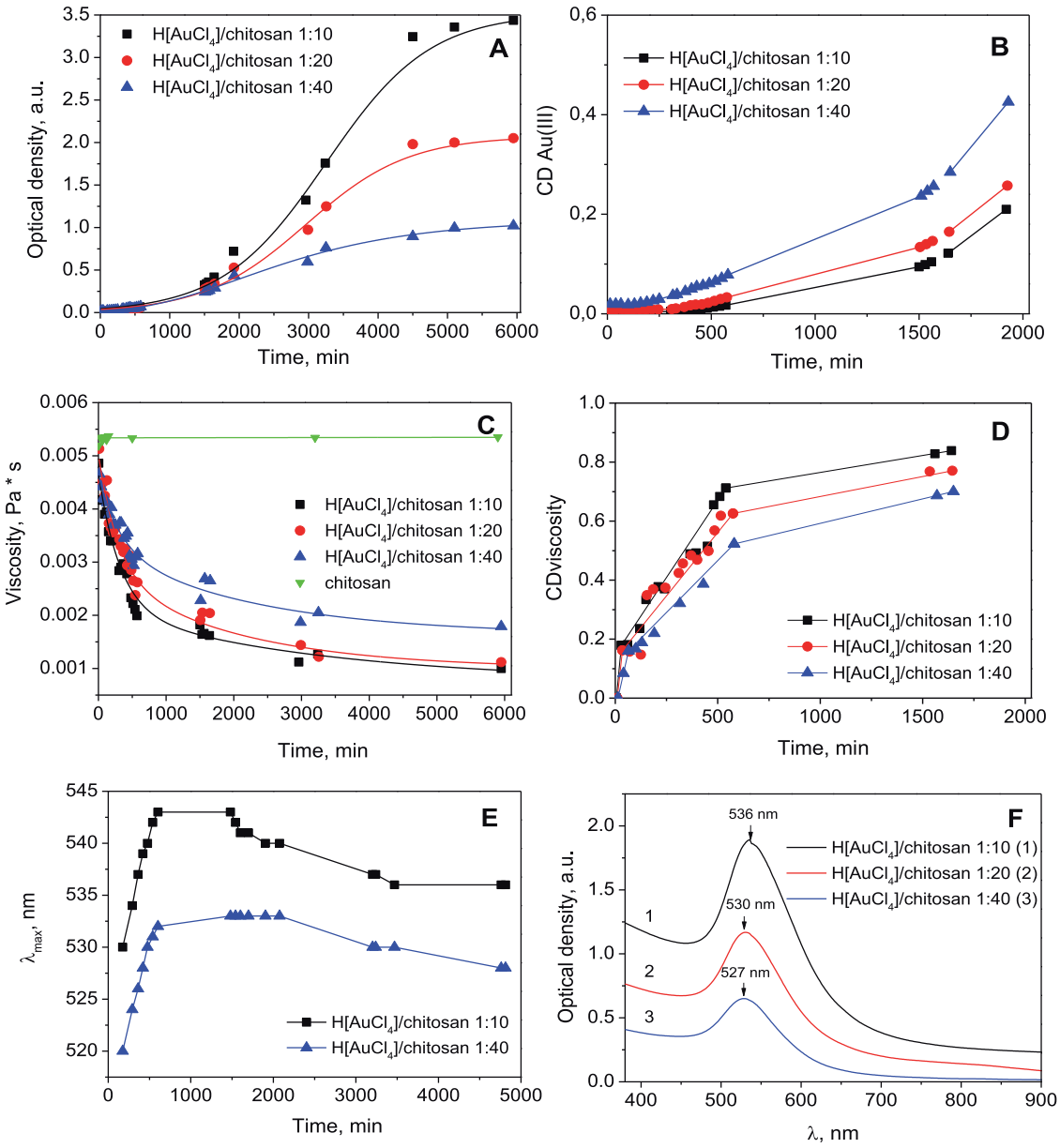

Fig. 1. Time dependences of optical density (A) and viscosity (C) in $H[AuCl_4]$/chitosan solutions and corresponding conversion degrees (B and D). Time-dependence of wavelength of gold nanoparticles plasmon absorption band (E) and spectra of chitosan/Au(0) composites after complete reduction of $H[AuCl_4]$ (F). (For interpretation of the references to color in this figure legend, the reader is referred to the web version of this article.)

accepted reaction mechanism of a glycosidic linkage hydrolysis (Einbu, Grasdalen, & Varum, 2007).

Au(III) coordination with chitosan is indeed crucial for glycosidic linkage hydrolysis, since formation of colloidal gold was not observed in 0.1 M HCl (Yu, Yang, Liu, & Chen, 2010) and even in more diluted HCl solutions—0.1% HCl (Fig.S2, Supporting materials) and in HCl solutions with pH 2–3 (Vo et al., 2014), i.e. when interactions occurred mainly via ion pairing of chitosan amino group with

Table 1
Mass balance of chitosan and products of its transformation.

Molar ratio $H[AuCl_4]$/chitosan	Weight loss of chitosan in composite (%)	Concentration of colloidal species (CS)[a] (meqv/L)		% (weight) of chitosan decomposed to	Molar ratio cationic/anionic CS	
		Cationic	Anionic	"cationic trash" (%)	LMW products (%)	
Chitosan		6.07 ± 0.07	0			
Chitosan/Au(0) composites						
1:80	1.01	0.037 ± 0.01	0.067 ± 0.02	0.59	0.4	0.54
1:40	3.96	0.10 ± 0.04	0.09 ± 0.06	2.37	1.6	1.56
1:20	13.45	0.39 ± 0.02	0.026 ± 0.01	6.42	7.0	15.00
1:10	48.69	1.26 ± 0.01	0.078 ± 0.01	20.75	27.9	16.15

[a] Content of cationic or anionic colloidal species (CS) in chitosan stock solution (0.1%) or in supernatant after precipitation of chitosan/Au(0) composite.

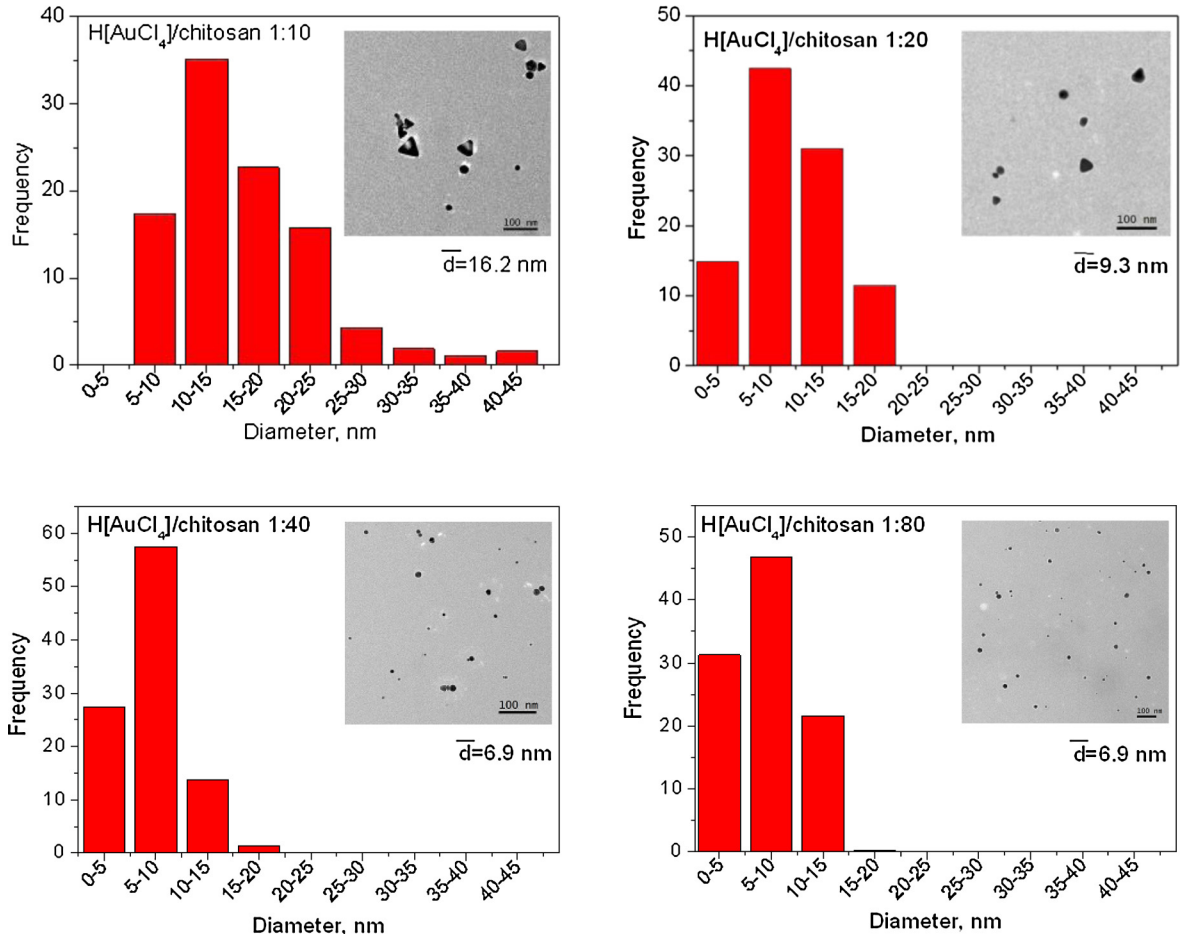

Fig. 2. TEM images of chitosan/Au(0) composites obtained at different $H[AuCl_4]$/chitosan ratios.

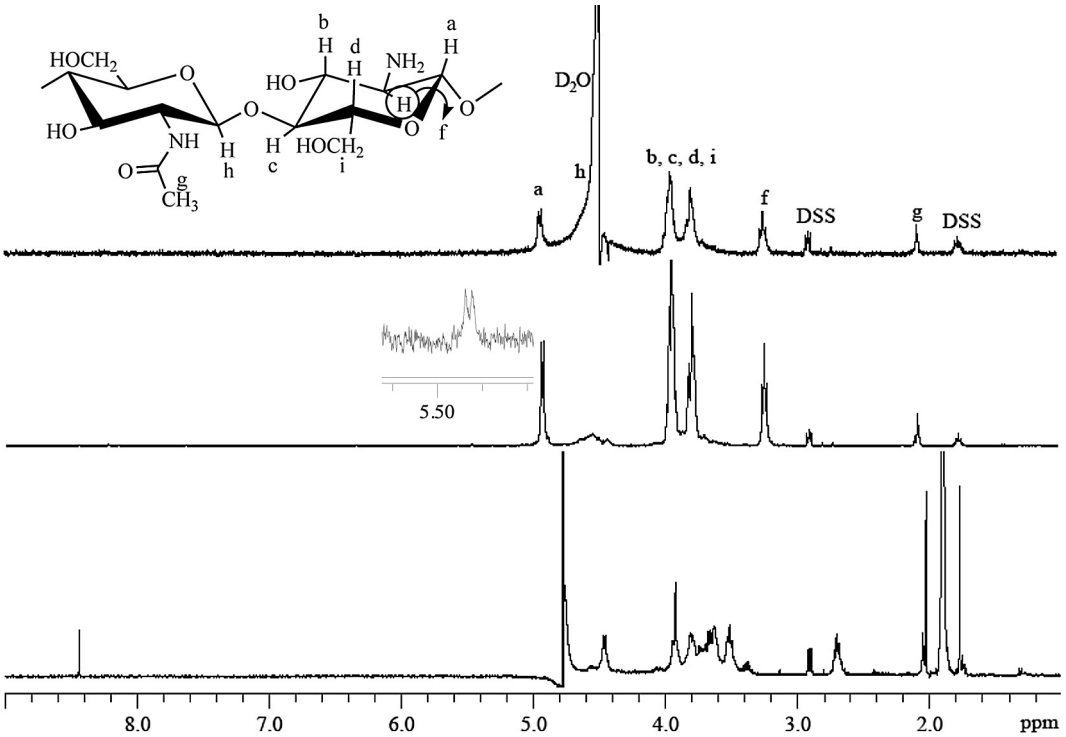

Fig. 3. ^1H NMR spectra (from top to bottom) of chitosan, chitosan/Au(0) composite and decomposition products in supernatant after precipitation and separation of chitosan/Au(0) composite (ratio 1:10).

$[AuCl_4]^-$ ion, which is most stable ionic specie under these conditions and is less effective oxidizer than other Au(III) ionic species existing at lower Cl^- concentrations (Sen Gupta, Pal, & Begum, 2001; Sen, Gani, Midya, & Pal, 2012).

Taking into account that Au (III) ions will preferably coordinate amino-groups rather than hydroxyl- or acetamido-groups (Afanas'eva, Glinskaya, Klevtsova, & Mironov, 2010; Cao, Jennings, & Puddephatt, 2007), glycoside linkages adjacent to deacetylated fragments will be hydrolyzed in the first place yielding glucosamine and its oligomers with acetylated terminating units. Other oligomeric structures (II, III, Scheme 1) can be formed at this stage. It was also previously shown that acid catalyzed hydrolysis of glycosidic linkage followed *N*-acetylated unit was three orders of magnitude faster as compared to glycosidic linkage following *N*-deacetylated unit (Varum, Ottoy, & Smidsrod, 2001). This can explain the increase of the acetylation degree from 0.12 for original chitosan to 0.26 for water-soluble oligochitosan detected in solution by ^{1}H NMR spectroscopy after Au(III) reduction to Au(0). The presence of cationic colloidal species—chitosan oligomers, which were not precipitated at pH 8 with chitosan/Au(0) composites, was also confirmed by colloid titration data (Table 1). Besides, the concentration of such fragments increases noticeably along with the increase of Au(III) concentration reaching the value of ~21% losses of chitosan weight to the water-soluble "cationic trash" at Au(III)\chitosan ratio 1:10 (Table 1).

The viscosimetry data (Fig. 1C and D) show that hydrolysis reaction is the most intensive within the first hours of Au(III)/chitosan interactions. However, fast development of purple-color, characteristic for colloidal gold, starts only when chitosan chain is substantially degraded and hydrolysis slows down (Fig. 1A and B). The latter clearly proves that not chitosan itself, but the products of its hydrolysis act as reducers in the reaction with Au(III). Similarly to the mechanism of Au(III) and Ag(I) reduction by β-D-glucose proposed in (Raveendran, Fu, & Wallen, 2003; Shervani & Yamamoto, 2011), Huang and Yang (2004) earlier hypothesized that D-glucosamine, as the main product of chitosan hydrolysis, can be the predominant reducing agent in chitosan solution but have not provided any supporting information.

Considering the literature data on Au(III) reduction by glucose derivatives (Sen Gupta et al., 2001) and chitosan (Sun et al., 2008), one can assume that hydrolysis products with terminal aldehyde groups (II, III, Scheme 1) are oxidized by Au(III) to derivatives of glucosamine acids (IV, V, Scheme 1), whose presence in solution is compatible with our ^{1}H NMR data (signals at 2.70–3.70 ppm, Fig. 3, Fig. S5, Supporting materials). One should mention that, although oxidation of aldehyde group at the C-1 position seems to be more probable reaction pathway, oxidation of hydroxyl group at the C-6 position cannot be excluded (Huang & Yang, 2004; Sen Gupta et al., 2001). This possibility is also supported by the literature data on Au(III) reduction with cellulose (Li, Friedrich, & Taubert, 2008). Besides, the colloid titration data show (Table 1) that at low Au(III) content (ratio 1:80) colloidal species of hypothetical structure V (Scheme 1) containing two carboxylic group per one amino-group dominate in solution.

However, at more advanced stages of oxidation with the increase of the Au(III) content, the "colloidal trash" has a predominantly cationic nature (Table 1). This suggests that glucosamine acids undergo further decarboxylation catalyzed by Au(III) ions. Formation of intermediate complexes with Au(III) (VI, Scheme 1), which decomposes to CO_2 and iminic cation (VII, Scheme 1), which is further rapidly hydrolyzed to aldehydes (VIII, Scheme 1) and NH_4^+ ions, is the most probable pathway, which was previously reported for aminoacids (Hussain & Ahmad, 1989; Sen et al., 2012; Sherigara, Bhat, Pinto, & Gowda, 1995). Although α-hydroxyacids (IX, Scheme 1), as the products of this reaction, cannot be identified by ^{1}H NMR analysis due to overlapping with chitosan signals, the formation of formic acid as a final product of oxidation was proved.

It is important to emphasize that the ratio formate/NH_2-group found in solution after precipitation of chitosan/Au(0) composite is very high—9:1 (for the systems with the Au(III)/chitosan ratio 1:10) indicating that a substantial part of chitosan decomposes into water-soluble low molecular weight products of non-colloidal nature. Formation of formic acid from hexoses and pentoses was previously reported in (Deng, Zhang, & Wang, 2014; Limacher, Kerler, Davidek, Schmalzried, & Blank, 2008), but have never been mentioned for chitosan/Au(III) systems.

The colloid titration data show (Table 1) that at the Au(III)/chitosan molar ratio 1:10 about 30% of chitosan is decomposed into low molecular weight (LMW) products. Such a significant decomposition of chitosan in Au(III) reduction process can explain a decrease of the apparent size of gold nanoparticles over time (Fig. 1E). Most likely, it results from the decrease of polymer shell thickness leading to blue-shift of plasmon adsorption band. The opposite effect—the red-shift of plasmon band is reported for gold nanoparticles after adsorption of polymer layer (Pal et al., 2005). Thus, degradation of chitosan macromolecule definitely decreases its efficiency as a stabilizer. Thinning of protective polymer layer can be an important factor leading to the increase of particle size and the formation of irregularly shaped gold nanoparticles at high metal loadings in chitosan/Au(0) composites as observed by TEM (Fig. 2).

4. Conclusions

The mechanism of Au(III) reduction by chitosan was investigated by combination of supplementary methods—UV–vis spectroscopy, rheology, transmission microscopy and ^{13}C and ^{1}H NMR spectroscopy. This is the first attempt to identify by-products of the redox reaction between chitosan and Au(III) and estimate how the Au(III)/chitosan ratio influences the resulting chemical composition of the system.

We show that Au(III) reduction in chitosan solution can be considered as a 3-stage process. It starts with complexation of Au(III) ion with chitosan leading to dissociation of $[AuCl_4]^-$complex. At the second stage, Au(III) ion as a strong Lewis acid catalyzes chitosan hydrolysis that becomes evident from drastic reduction of viscosity. This period roughly coincides with the induction period of Au(III) reduction, when the development of purple color typical for colloidal gold is very slow. Only when hydrolysis slows down and sufficient amount of hydrolysis products is accumulated, the third stage of fast Au(III) reduction to Au(0) particles starts. This indicates that not chitosan itself, but the products of its hydrolysis are the main reducing agents in $H[AuCl_4]$/chitosan solutions. According to ^{13}C and ^{1}H NMR spectroscopy data, the chitosan reaction with Au(III) leads to its decomposition into chitosan oligomers, derivatives of glucosamine acids, and formate. The decrease of chitosan molecular weight and its oxidative degradation rather than the formation and rupture of chitosan/gold nanoparticle bonds is the most probable reason for self-collapsing of chitosan/Au(0) gels recently observed in (Ramasamy & Maliyekkal, 2014).

The rate of Au(III) reduction and characteristics of the nanoparticles formed significantly depend on the Au(III)/chitosan molar ratio. Hydrolytic and oxidative destruction of chitosan, which is enhanced by increasing Au(III) concentration, reduces the stabilizing efficiency of chitosan, hence, gold nanoparticles formed at Au(III)/chitosan molar ratio above 1:40 have bigger sizes, higher polydispersity, and are irregularly shaped.

The advantage of chitosan as reducing agent is often seen in its biocompatibility, which allows using chitosan/Au(0) composites without purification (Murugadoss & Sakurai, 2011; Ramasamy

& Maliyekkal, 2014) even in the biomedical field (Ramasamy & Maliyekkal, 2014). However, biocompatibility and non-toxicity of chitosan/Au(0) composites has to be considered taking into account the biological activity of the by-products formed. For example, retinal photoreceptors and retinal pigment epithelial cells are sensitive to poisoning with formic acid (Treichel, Henry, Skumatz, Eells, & Burke, 2004), which is formed in significant quantities upon chitosan oxidation with Au(III), as we have shown here.

Acknowledgment

Financial support from Russian Scientific Foundation (project no 14-13-00136) is gratefully acknowledged.

Appendix A. Supplementary data

Supplementary data associated with this article can be found, in the online version, at http://dx.doi.org/10.1016/j.carbpol.2014.09.030.

References

Afanas'eva, V. A., Glinskaya, L. A., Klevtsova, R. F., & Mironov, I. V. (2010). Dinuclear complex of gold(III) with 1,3-diaminopropane (HL), $[Au_2(HL)(L)_2](ClO_4)_3(OH)$: Synthesis and crystal and molecular structures. *Russian Journal of Coordination Chemistry*, *36*, 697–703.

Agrawal, P., Strijkers, G. J., & Nicolay, K. (2010). Chitosan-based systems for molecular imaging. *Advanced Drug Delivery Reviews*, *62*, 42–58.

Braier, N. C., & Jishi, R. A. (2000). Density functional studies of Cu^{2+} and Ni^{2+} binding to chitosan. *Journal of Molecular Structure: THEOCHEM*, *499*, 51–55.

Cao, L., Jennings, M. C., & Puddephatt, R. J. (2007). Amine–amide equilibrium in gold(III) complexes and a gold(III)–gold(I) aurophilic bond. *Inorganic Chemistry*, *46*, 1361–1368.

Chen, Z., Wang, Z., Chen, X., Xu, H., & Liu, J. (2013). Chitosan-capped gold nanoparticles for selective and colorimetric sensing of heparin. *Journal of Nanoparticle Research*, *15*, 1930 (UNSP)

Deng, W., Zhang, Q., & Wang, Y. (2014). Catalytic transformations of cellulose and cellulose-derived carbohydrates into organic acids. *Catalysis Today*, *234*, 31–41.

Di Carlo, G., Curulli, A., Toro, R. G., Bianchini, C., De Caro, T., Padeletti, G., et al. (2012). Green synthesis of gold-chitosan nanocomposites for caffeic acid sensing. *Langmuir*, *28*, 5471–5479.

Djoković, V., Božanic, D. K., Vodnik, V. V., Krsmanović, R. M., Trandafilovic, L. V., & Dimitrijević-Branković, S. (2011). Structure and optical properties of noble-metal and oxide nanoparticles dispersed in various polysaccharide biopolymers. *Proceedings of SPIE*, *8098*, 809–816.

Einbu, A., Grasdalen, H., & Varum, K. (2007). Kinetics of hydrolysis of chitin/chitosan oligoniers in concentrated hydrochloric acid. *Carbohydrate Polymers*, *342*(8), 1055–1062.

Huang, H., & Yang, X. (2004). Synthesis of chitosan-stabilized gold nanoparticles in the absence/presence of tripolyphosphate. *Biomacromolecules*, *5*, 2340–2346.

Huang, H., Yuan, Q., & Yang, X. (2004). Preparation and characterization of metal-chitosan nanocomposites. *Colloids and Surfaces B: Biointerfaces*, *39*, 31–37.

Hussain, M. Y., & Ahmad, F. (1989). A comparative kinetic and mechanistic study of glutamic acid oxidation by acid permanganate in the absence and presence of sodium dodecyl sulphate. *Transition Metal Chemistry*, *14*, 169–174.

Khlebtsov, N. G. (2008). Determination of size and concentration of gold nanoparticles from extinction spectra. *Analytical Chemistry*, *80*, 6620–6625.

Kumar, V., & Yadav, S. K. (2009). Plant-mediated synthesis of silver and gold nanoparticles and their applications. *Journal of Chemical Technology and Biotechnology*, *84*, 151–157.

Li, Z., Friedrich, A., & Taubert, A. (2008). Gold microcrystal synthesis via reduction of HAuCl4 by cellulose in the ionic liquid 1-butyl-3-methyl imidazolium chloride. *Journal of Materials Chemistry*, *18*, 1008–1014.

Limacher, A., Kerler, J., Davidek, T., Schmalzried, F., & Blank, I. (2008). Formation of furan and methylfuran by Maillard-type reactions in model systems and food. *Journal of Agricultural and Food Chemistry*, *56*, 3639–3647.

Mayer, A. B. R., & Mark, J. E. (1998). Colloidal gold nanoparticles protected by water-soluble homopolymers and random copolymers. *European Polymer Journal*, *34*, 103–108.

Murugadoss, A., & Sakurai, H. (2011). Chitosan-stabilized gold, gold–palladium, and gold–platinum nanoclusters as efficient catalysts for aerobic oxidation of alcohols. *Journal of Molecular Catalysis A: Chemical*, *341*, 1–6.

Pal, A., Esumi, K., & Pal, T. (2005). Preparation of nanosized gold particles in a biopolymer using UV photoactivation. *Journal of Colloid and Interface Science*, *288*, 396–401.

Park, Y., Hong, Y. N., Weyers, A., Kim, Y. S., & Linhardt, R. J. (2011). Polysaccharides and phytochemicals: A natural reservoir for the green synthesis of gold and silver nanoparticles. *IET Nanobiotechnology*, *5*, 69–78.

Pretsch, E., Bühlmann, P., & Affolter, C. (2000). *Structure determination of organic compounds: Tables of spectral data*. Berlin: Springer.

Ramasamy, R. P., & Maliyekkal, S. M. (2014). Formation of gold nanoparticles upon chitosan leading to formation and collapse of gels. *New Journal of Chemistry*, *38*, 63–69.

Raveendran, P., Fu, J., & Wallen, S. L. (2003). Completely green synthesis and stabilization of metal nanoparticles. *Journal of American Chemical Society*, *125*, 13940–13941.

Schneider, C. A., Rasband, W. S., & Eliceiri, K. W. (2012). NIH image to ImageJ: 25 years of image analysis. *Nature Methods*, *9*, 671–675.

Sen Gupta, K. K., Pal, B., & Begum, B. A. (2001). Reactivity of some sugars and sugar phosphates towards gold(III) in sodium acetate–acetic acid buffer medium. *Carbohydrate Research*, *330*, 115–123.

Sen, P. K., Gani, N., Midya, J. K., & Pal, B. (2012). Effects of nonionic micellar aggregates on the electron transfer reaction between L-glutamic acid and gold(III) complexes. *International Journal of Chemical Kinetics*, *44*, 482–493.

Sherigara, B. S., Bhat, K. I., Pinto, I., & Gowda, N. M. M. (1995). Oxidation of L-aspartic acid and L-glutamic acid by manganese(III) ions in aqueous sulfuric acid, acetic acid, and pyrophosphate media—A kinetic study. *International Journal of Chemical Kinetics*, *27*, 675–690.

Shervani, Z., & Yamamoto, Y. (2011). Carbohydrate-directed synthesis of silver and gold nanoparticles: Effect of the structure of carbohydrates and reducing agents on the size and morphology of the composites. *Carbohydrate Research*, *346*, 651–658.

Soriano, E., & Marco-Contelles, J. (2011). *Structure, bonding, and reactivity of reactant complexes and key intermediates. Computation mechanisms of Au and Pt catalized reactions Topics in current chemistry* (302) Berlin: Springer-Verlag.

Sun, C. M., Qu, R. J., Chen, H., Ji, C. N., Wang, C. H., Sun, Y., et al. (2008). Degradation behavior of chitosan chains in the 'green' synthesis of gold nanoparticles. *Carbohydrate Research*, *343*, 2595–2599.

Tiwari, A. D., Mishra, A. K., Mishra, S. B., Arotiba, O. A., & Mamba, B. B. (2011). Green synthesis and stabilization of gold nanoparticles in chemically modified chitosan matrices. *International Journal of Biological Macromolecules*, *48*, 682–687.

Treichel, J. L., Henry, M. M., Skumatz, C. M. B., Eells, J. T., & Burke, J. M. (2004). Antioxidants and ocular cell type differences in cytoprotection from formic acid toxicity in vitro. *Toxicological Science*, *82*, 183–192.

Varum, K. M., Ottoy, M. H., & Smidsrod, O. (2001). Acid hydrolysis of chitosans. *Carbohydrate Polymers*, *46*(1), 89–98.

Vo, K. D. N., Guillon, E., Dupont, L., Kowandy, C., & Coqueret, X. (2014). Influence of Au(III) interactions with chitosan on gold nanoparticle formation. *Journal of Physical Chemistry C*, *118*(8), 4465–4474.

Whittall, J., & Sutton, P. (2009). *Practical methods for biocatalysis and biotransformations*. New York: Willey.

Wu, Y., Zuo, F., Lin, Y., Zhou, Y., Zheng, Z., & Ding, X. (2014). Green and facile synthesis of gold nanoparticles stabilized by chitosan. *Journal of Macromolecular Science, A: Pure and Applied Chemistry*, *51*, 441–446.

Yu, C.-C., Yang, K.-H., Liu, Y.-C., & Chen, B.-C. (2010). Photochemical fabrication of size-controllable gold nanoparticles on chitosan and their application on catalytic decomposition of acetaldehyde. *Materials Research Bulletin*, *45*, 838–843.

Zhang, G., Sun, X., Jasinski, J., Patel, D., & Gobin, A. M. (2012). Gold/chitosan nanocomposites with specific near infrared absorption for photothermal therapy applications. *Journal of Nanomaterials*, *2012*, 853416.